PNAS RESEARCH ARTICLE | DEVELOPMENTAL BIOLOGY

Direct and indirect gene repression by the ecdysone cascade during mosquito reproductive cycle

Sourav Roy[a,b,1,2], Tusar T. Saha[c,1,2], Jisu Ha[a,d], Roumik Banerjee[c], Emre Aksoy[a,d], Aditi Kulkarni[b], and Alexander S. Raikhel[a,2]

Contributed by Alexander S. Raikhel; received September 23, 2021; accepted January 27, 2022; reviewed by Daniel McKay and Jinsong Zhu

Hematophagous mosquitoes transmit devastating human diseases. Reproduction of these mosquitoes is cyclical, with each egg maturation period supported by a blood meal. Previously, we have shown that in the female mosquito *Aedes aegypti*, nearly half of all genes are differentially expressed during the postblood meal reproductive period in the fat body, an insect analog of mammalian liver and adipose tissue. This work aims to decipher how transcription networks govern these genes. Bioinformatics tools found 89 putative transcription factor binding sites (TFBSs) on the *cis*-regulatory regions of more than 1,400 differentially expressed genes. Putative transcription factors that may bind to these TFBSs were identified and used for the construction of temporally coordinated regulatory networks. Further molecular biology analyses have uncovered mechanisms of direct and indirect negative transcriptional regulation by the steroid hormone 20-hydroxyecdysone (20E) through the ecdysone receptor (EcR). Genes within the two groups, early genes and late mid-genes, have distinctly different expression profiles. However, both groups of genes show lower expression at the high titers of 20E and are down-regulated by the 20E/EcR cascade by different molecular mechanisms. Transcriptional repression of early genes is indirect and involves the classic 20E pathway with ecdysone-induced protein E74 functioning as a repressor. Late mid-genes are repressed directly by EcR that recognizes and binds a previously unreported DNA element, different from those utilized in the 20E-mediated gene activation, within the regulatory regions of its target genes and recruits Mi2 that acts as a corepressor, initiating chromatin condensation.

ecdysone receptor | gene repression | corepressor

Significance

Hematophagous *Aedes aegypti* mosquitoes spread devastating viral diseases. Upon blood feeding, a steroid hormone, 20-hydroxyecdysone (20E), initiates a reproductive program during which thousands of genes are differentially expressed. While 20E-mediated gene activation is well known, repressive action by this hormone remains poorly understood. Using bioinformatics and molecular biological approaches, we have identified the mechanisms of 20E-dependent direct and indirect transcriptional repression by the ecdysone receptor (EcR). While indirect repression involves E74, EcR binds to an ecdysone response element different from those utilized in 20E-mediated gene activation to exert direct repressive action. Moreover, liganded EcR recruits a corepressor Mi2, initiating chromatin compaction. This study advances our understanding of the 20E-EcR repression mechanism and could lead to improved vector control approaches.

The *Aedes aegypti* mosquito is the primary vector for viruses that belong to the Flaviviridae family, causing severe human diseases, including dengue, yellow fever, chikungunya, and Zika (1–3). Vector control is the primary option for prevention of diseases inflicted by dengue and Zika viruses due to the unavailability of vaccines. *Ae. aegypti* is an outstanding model for studying anautogenous insect vectors because the reproductive events occur within a short time span and are highly synchronized with blood feeding. The cyclical nature of reproductive events in female mosquitoes serve as a foundation for pathogen transmission, making it an important phenomenon for research.

In a previous transcriptome-wide study, we have reported that nearly half of all transcripts are differentially expressed in temporally distinct patterns during the postblood meal (PBM) reproductive period in the fat body (FB) of a female *Ae. aegypti* mosquito (4). We also identified the major regulators for each of these patterns and demonstrated that there is a correlation between the titers of the two insect hormones, juvenile hormone (JH) and 20-hydroxyecdysone (20E), and the gene-expression patterns. Of the four broad groups of genes—namely early genes (EGs), early mid-genes (EMGs), late mid-genes (LMGs), and late genes (LGs)—expressions of the those within the first three groups were affected by 20E. While representatives of EMGs were activated, that from EGs and LMGs were down-regulated at the high titer of 20E, between 18 and 24 h PBM (*SI Appendix*, Fig. S1*A*). However, the expression patterns of genes within these two groups were markedly different. EGs reached the maximum levels of expression between 6 and 12 h PBM, while the LMGs were between 36 and 48 h PBM.

The molecular biology of 20E regulatory action has been researched in considerable detail (5). However, until recently, most of these studies focused on positive regulation by the ecdysone receptor (EcR), in the presence of 20E, including those controlling vitellogenesis in *Ae. aegypti* (6, 7). EcR is conventionally thought to function as a repressor in the absence of hormone; however, we provided preliminary evidence in our previous study that EcR may also be involved in the negative regulation of transcripts, in the presense of 20E, during the PBM reproductive period in *Ae. aegypti* (4). Since then, other studies have also reported a direct and widespread role of EcR in regulating tissue-specific transcriptional programs in *Drosophila* development (8, 9),

Author contributions: S.R., T.T.S., and A.S.R. designed research; S.R., T.T.S., J.H., R.B., E.A., and A.K. performed research; S.R., T.T.S., J.H., R.B., E.A., and A.K. contributed new reagents/analytic tools; S.R., T.T.S., and A.S.R. analyzed data; and S.R., T.T.S., and A.S.R. wrote the paper.

Reviewers: D.M., University of North Carolina at Chapel Hill College of Arts and Sciences; and J.Z., Virginia Polytechnic Institute and State University.

The authors declare no competing interest.

[1]S.R. and T.T.S. contributed equally to this work.

[2]To whom correspondence may be addressed. Email: sroy1@utep.edu, tusars@goa.bits-pilani.ac.in, or alexander.raikhel@ucr.edu.

This article contains supporting information online at http://www.pnas.org/lookup/suppl/doi:10.1073/pnas.2116787119/-/DCSupplemental.

Published March 7, 2022.

suggesting that it may not be an isolated phenomenon related to mosquito reproduction. This prompted us to investigate the molecular mechanism of the 20E-mediated repressive action in the presence of 20E in *Ae. aegypti*.

Gene expression through activation or inhibition is determined by transcription factors (TFs) recognizing their cognate binding sites, *cis*-regulatory elements (CREs), in regulatory regions and promoter sequences of a gene (10). Thus, identifying CREs can lead to the discovery of their corresponding TFs, aiding in understanding the mechanism behind the expression profile of a particular gene. Therefore, as a first step in our investigation we employed bioinformatics tools for the identification of CREs in differentially expressed gene sets in the mosquito FB, which we believe along with their corresponding TFs are involved in the formation of gene regulatory networks during the reproductive period in female mosquitoes. Putative regulatory networks were built using the protein–protein interaction data available from *Drosophila*. For functional analyses, we selected the networks for two gene clusters, EGs and LMGs, where transcripts display a minimum level of expression between 18 and 24 h PBM when the titer of 20E is at its peak (*SI Appendix*, Fig. S1*A*). Representatives of both clusters have previously been found to be negatively regulated by 20E through the EcR (4).

Our analyses have revealed a striking difference in molecular mechanisms governing 20E/EcR-mediated repression of EGs and LMGs. Negative regulation of members of the former gene set is indirect and involves the classic 20E pathway with the B isoform of the ecdysone induced protein (E74B) functioning as a repressor. In contrast, we have identified a unique sequence (TTGATTGA) that is involved in direct repression of the representatives of the LMGs by EcR. Genes with this motif in their *cis*-regulatory regions (CRRs) were derepressed following the RNA interference (RNAi)-mediated depletion of EcR. Tests with cycloheximide (CHX) suggested that no intermediate factors were required for the 20E-mediated repression of genes with this ecdysone responsive element specific for repression (EcREr) within their CRRs. Chromatin immunoprecipitation (ChIP) and electrophoretic mobility shift assays (EMSA) have confirmed that the A isoform of the EcR protein (EcR-A) interacts with the specific EcREr DNA element in the CRRs of the target LMGs. RNAi-mediated depletion showed that Ultraspiricle (USP), the heterodimeric partner of EcR, has no role in the 20E/EcR-mediated direct repression of the LMG transcripts. Instead, *Aa*Mi2, a corepressor, is recruited as a component of the 20E/EcR complex that binds to EcREr to mediate gene repression by chromatin compaction of target gene loci.

Results

Discovery of Putative TF Binding Sites Provides an Insight into Temporal Transcriptional Regulatory Networks.

Identification of overrepresented motifs displayed cluster specificity. The noncoding genomic regions are essential for gene regulation and genome complexity (11). One of the goals of this study was to look for CREs within the intergenic regions of the *Ae. aegypti* (12). We searched for the intergenic regions and observed that there are at least three times more genes with intergenic regions of 2 kb or less (includes gene pairs both in 5′ to 3′ and 3′ to 5′ directions) when compared to the numbers in any other 2-kb window (*SI Appendix*, Fig. S1*B*). We also found that the average length of 5′ UTR in the transcripts (~55% of the total number of transcripts had annotated 5′ UTRs) is 229 bases with more than 60% having a 5′ UTR of 200 bases or less (*SI Appendix*, Fig. S1*C*).

We have used the gene-expression data from our previous study (4) to select genes coexpressed at different times during the PBM period. We investigated genes from all four groups: namely, EGs (clusters 1 and 6), EMGs (clusters 4 and 7), LMGs (cluster 5), and LGs (clusters 2A and 2B). The clusters were the same as in the original clustering (4), and the largest cluster (cluster 2) was divided into two clusters. Approximately 200 genes were selected from each cluster based on the maximum $\log_2$ fold-change ($\log_2$ FC) in their expression values and their similarity to the average expression profile of a particular cluster (Dataset S1). The CRRs of *Ae. aegypti* genes (2-kb upstream regions from the translation start sites, ATG), were extracted with the information regarding the start positions obtained from the general feature format (GFF3) files. This step resulted in seven datasets with ~200 CRRs in each set (12), and each CRR with a maximum of 2,000 bp.

The datasets generated in the previous step were used as inputs for the two different motif-finding programs (*SI Appendix*, Fig. S2). MEME (13), based on expectation maximization, identified up to 100 motifs for each set, between the lengths of 6 and 9 bp. On the other hand, Weeder and colleagues (14), with a de novo motif discovery program evaluating the statistical significance of k-mers, identified the top 50, 6-bp and 8-bp motifs. The intersection between the motifs detected by the two programs was checked, and in some cases, similar motifs were merged allowing 2-bp degeneracy. *SI Appendix*, Table S1 lists the final set of motifs that were identified by both programs. The number of motifs in each cluster ranged from a minimum of 5 to a maximum of 22 (*SI Appendix*, Table S1). Each of these motifs, were subjected to the test of equality of proportions against a randomly generated set of CRRs. All the motifs detected passed this test. To check for cluster specificity, a hypergeometric test was applied. The results, when plotted with the *P* values from the hypergeometric test as a heatmap (Fig. 1), showed a clear demarcation between the motifs from each cluster even though some motifs were overrepresented in more than one cluster.

Detection of positional and orientation biases, and evolutionary conservation, resulted in identification of putative TF binding sites. Many transcription factors act at a certain distance from the transcription start site (TSS) or other regulatory locations, and this distance seem to be important for the functioning of these factors. Therefore, it is expected that their corresponding TF biding sites (TFBSs) would be concentrated at a certain site within the promoter space (15). In order to check whether a motif shows positional bias, the frequencies for occurrences of a motif within each of the 10 200-bp bins (that the 2-kb upstream regions were broken into) was checked (*SI Appendix*, Fig. S2). Datasets S2–S5 show the raw frequency of the overrepresented motifs in 5′ to 3′ and 3′ to 5′ directions along with the *P* values from the statistical tests for each of the seven clusters. The results of positional bias (*P* value cutoff < 0.01) analysis are shown in the "posi." column in Fig. 1. About 48% of the overrepresented motifs were found to display positional bias for one or more regions within the promoters.

Orientation (5′-3′ or 3′-5′) is important for certain TFs to fulfill their regulatory function; as a result, the corresponding TFBSs display a bias for a certain orientation. To check the orientation bias, the frequencies of motifs observed in the forward (5′ to 3′) and the reverse (3′ to 5′) directions were calculated. The results of the orientation bias (χ^2 test) are shown in the "orient." column of Fig. 1 and in Datasets S2–S5. These results

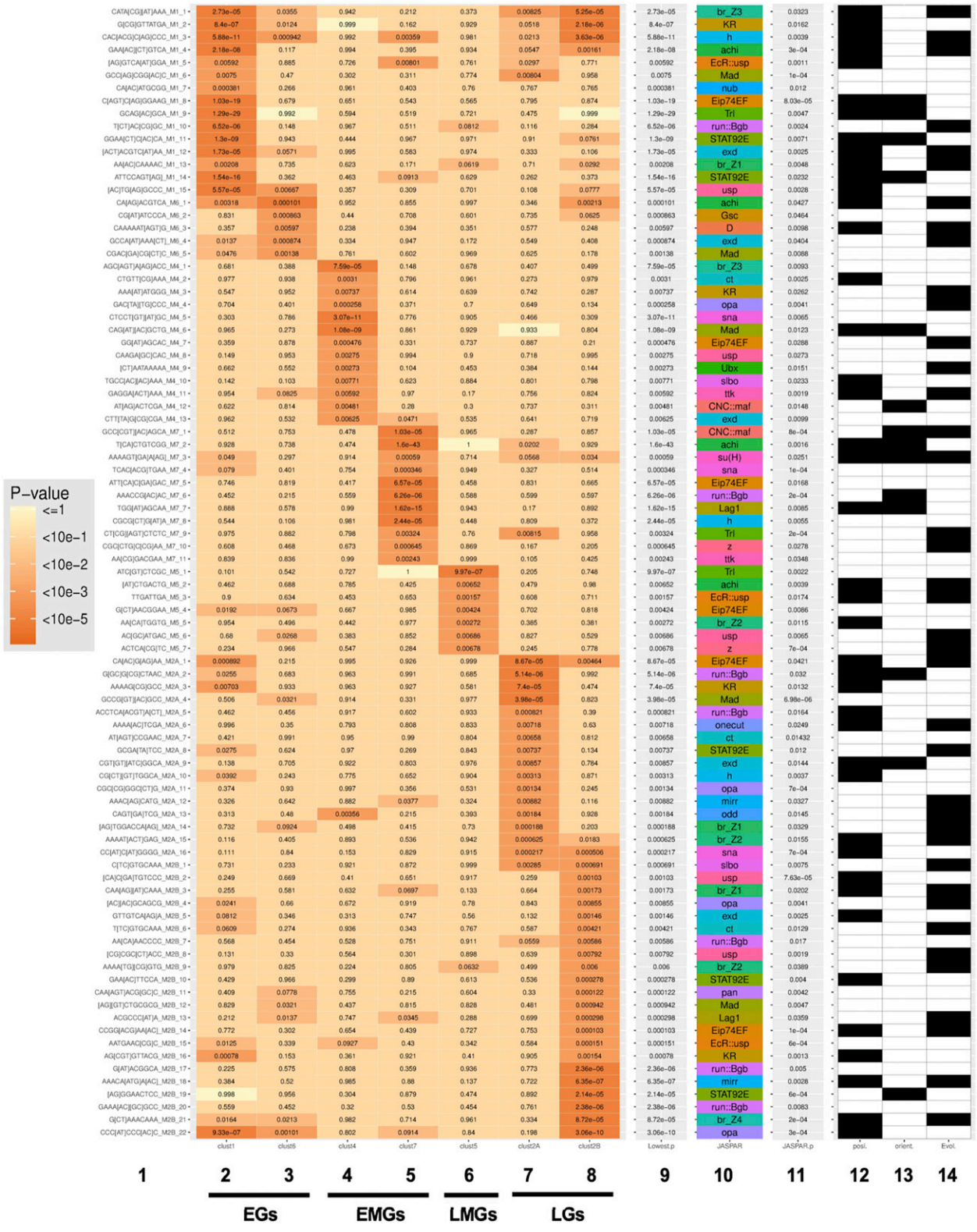

Fig. 1. Computational discovery of overrepresented motifs displays a clear demarcation between different groups of genes expressed during the mosquito vitellogenic cycle. Overrepresented motifs within the CRRs of genes in seven clusters: two of each from EGs, EMGs, and LGs, and one from LMGs, shown in column 1; *P* values for overrepresentation of motifs in each cluster calculated by hypergeometric test are shown in the form of heat map (columns 2–8), darker shade indicates lower *P* value; the lowest *P* value (Lowestp) from the hypergeometric test for each motif is shown in column 9; putative TF for each motif detected from JASPAR database is shown in column 10; column 11 shows *P* value (cutoff of 0.01; TOMTOM comparison tool) for the TF matches; positional bias for each motif detected by the test of equality of proportions is shown in column 12; orientation bias determined by χ^2 test is shown in column 13, evolutionary conservation determined by aligning *Ae. aegypti* promoters with the respective orthologs in *An. gambiae* and *C. quinquefasciatus,* shown in column 14; dark shading indicates the detection of positional bias, orientation bias, and evolutionary conservation.

suggest that about 16% of the motifs displayed orientation bias, and most (~70%) that showed orientation bias also displayed positional bias.

Comparative genomics also offers methods for predicting motifs by searching cross-species promoter alignments for phylogenetic footprints (i.e., regions of conservation) (16). This is because conserved noncoding sequences are often reliable guides to regulatory elements (17). We first selected the genes in which a particular motif appeared; preference was given to the region of positional bias. Their orthologs were identified in *Anopheles gambiae* and *Culex quinquefasciatus*, and 2-kb upstream CRRs were extracted and aligned with the multiple sequence alignment program MUSCLE (18). For each motif, a maximum of five genes and their orthologs were checked. Thirty-nine of the overrepresented motifs were found to be evolutionarily conserved in the orthologous genes of either one or both mosquito species (Fig. 1 and Datasets S2–S5). Nine motifs from the EG, 9 from the EMG, 4 from the LMG, and 17 from the LG clusters were found to be conserved. Approximately 50% of the conserved motifs also displayed positional bias (Fig. 1 and Datasets S2–S5).

Identification of TFs corresponding to the putative TFBSs, and determination of tissue specificity, led to construction of cluster-specific putative regulatory networks. Our next step was to identify the TFs corresponding to each of the putative TFBSs identified within the promoters of the cluster-specific, coregulated transcripts. The TOMTOM motif comparison tool (https://meme-suite.org/meme/tools/tomtom) was used to map the overrepresented motifs onto known transcription factors in the JASPAR database (19). The TOMTOM program confirmed similarities using a P value cutoff < 0.01. List of probable transcription factors were obtained from JASPAR search for each cluster (Datasets S2–S5). TFs obtained from JASPAR was used to examine the FlyAtlas2 database (www.www.flyatlas.org/atlas.cgi) (20) for tissue-specific expression of *Drosophila* TFs. From all detected TFs, we identified those expressed in *Drosophila* FB tissue. A P value cutoff of 0.01 was used for this purpose. Once the tissue-specificity was determined, a final list of TFs was obtained (Fig. 1). Eighty-nine overrepresented motifs were mapped to 34 known TFs that have been shown to be expressed in the *Drosophila* FB.

Now that we had identified the TFs, we decided to explore those related to 20E negative regulatory cascade. We focused on the two groups of genes, EGs and LMGs, that were downregulated at the 20E high titer. We built putative transcriptional networks using GeneMANIA (21) with the TFs identified by JASPAR, that were related to EG and LMG clusters (clusters 1 and 5, respectively) (*SI Appendix*, Fig. S3 *A* and *B* and Table S2).

20E-EcR–Mediated Repression of EGs Is Indirect and Occurs through E74.

Putative transcriptional network suggests 20E/EcR mediated repression is through E74. A JASPAR insecta database search with cluster1 motifs resulted in identification of 15 unique TFs (Fig. 1). Only six of these motifs passed two of the three bioinformatics tests discussed in the previous section. A JASPAR search suggested that these were putative TFBSs for the following TFs: Achintya (Achi), ecdysone-induced protein 74EF (Eip74EF), Trithorax-like (Trl), Homeobox protein extradenticle (Exd), Broad complex isoform Z1 (BR-Z1), and Signal-transducer and activator of transcription protein at 92E Stat92E (STAT) (Fig. 1). We checked how these transcription factors are linked to EcR within the regulatory network, built using GeneMANIA (*SI Appendix*, Fig. S3*A*).

Of the six TFs mentioned above, Stat92E, Achi, and BR displayed direct connections to EcR within the network, whereas Trl and Exd did not show any direct connection (*SI Appendix*, Fig. S3*A*). Two TFs—Mothers against decapentaplegic (Mad) and Nubbin (Nub)—were linked directly to EcR within the network, but the putative TFBSs for these factors did not test positive for any of the bioinformatics tests (Fig. 1) and hence were not studied further. Eip74EF (E74) did not show any direct connection but was linked to EcR through BR. Activation of the early-response genes within the 20E regulatory hierarchy, like E74, requires prior expression of BR complex proteins as the EcR protein complex is not sufficient (22). The E74 gene is located within the *Drosophila* E74EF puff (23), and in *Ae. aegypti* it is known to play crucial roles at different time points during the PBM phase (24, 25). E74 is one of the downstream genes in the 20E regulatory cascade, involved in regulation of 20E target genes. E74 has been shown to serve a repressor of a subset of secondary ecdysone targets (23). Shlyueva et al. (26) suggested that repression of enhancer activity after ecdysone treatment may be independent of EcR motifs but involves E74 motifs. Therefore, we checked the effects of EcR depletion on BR and E74.

E74 is activated by EcR in the presence of 20E through BR. We examined the effects of RNAi-mediated depletion of *EcR* (iEcR) and the control *Luciferase* (iLuc) on the *BR* and *E74* transcripts (Fig. 2 *A* and *B*). Significant decline in the transcript levels of both *BR* and *E74* confirmed the activation of these factors in the 24 h PBM FB tissue (Fig. 2 *A* and *B*). RNAi depletion of *BR* also resulted in the decline of *E74* transcript expression (Fig. 2*C*), suggesting that *E74* is activated by 20E/EcR through *BR* in mosquito FB at 24 h PBM.

E74-B is responsible for repression of EGs. Next, we tested the effects of EcR and Luc RNAi depletions on candidate E74 target genes. We selected two E74 target genes, *Sideroflexin-1* (*AAEL014526*) and *pancreatic lipase-related protein 2* (*AAEL008222*), that carry the E74 binding motifs within their CRRs, 1,850 to 2,000 bases upstream of the translation start site. A positional bias for the region between 1,800 and 2,000 bases upstream of ATG was detected for this motif. In addition, these genes were selected because along with being significantly differentially expressed, their expression profiles were very similar to that of the average expression profile of this group of genes (*SI Appendix*, Fig. S3*C*). We examined if E74, is responsible for negative regulation of these genes.

First, we tested the effect of E74 knockdown on these EGs. There was a significant increase in the level of transcripts for both the genes (Fig. 3*A* and *SI Appendix*, Fig. S4*A*) when compared to the control iLuc, suggesting that they are being negatively regulated by E74. Since BR activates E74, and E74 negatively regulates these EGs, then a knockdown of *BR* should result in a decrease of E74 levels followed by an increase in the level of transcripts of the target genes. The results confirmed that these target genes are de-repressed in the *BR* depleted 24-h PBM FB tissues (Fig. 3*B* and *SI Appendix*, Fig. S4*B*).

Similarly, because EcR is responsible for activation of E74 through BR, the depletion of EcR should have effects like that of BR depletion on the E74 target genes. We checked the expression of E74 target genes in *EcR*-depleted tissue, and the results showed an increase in the transcript levels of target genes (Fig. 3*C* and *SI Appendix*, Fig. S4*C*), suggesting that depletion of *EcR* results in a decrease of the E74 levels, which in turn results in de-repression of its target genes. Next, we utilized CHX, a potent translational inhibitor, in the in vitro FB culture (IVFBC) according to Saha et al. (27) to test the necessity

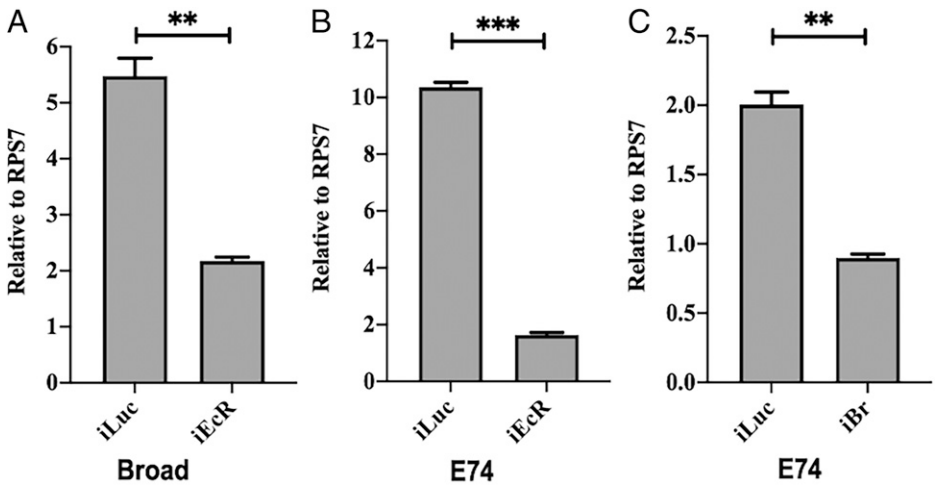

Fig. 2. Investigation of key components within the EG regulatory network of TFs: (*A* and *B*) RNAi depletion of EcR results in the down-regulation of the BR (*A*) and E74 (*B*) transcripts, suggesting an activation of these genes by 20E/EcR. Expressions relative to RPS7 detected by qRT-PCR, in the FB tissue collected from female mosquitoes after knockdown of EcR (iEcR). (*C*) RNAi depletion of BR results in the down-regulation of the E74 transcript. Expressions relative to RPS7 detected by qRT-PCR, in FB tissues collected from female mosquitoes after knockdown of BR (iBr). (*A–C*) Injecting double stranded RNA for the *Luciferase* gene (iLuc) served as a control for all RNAi experiments. Data representative of three biological replicates, with three technical replicates and are illustrated as average ± SD, ***P* value < 0.01, ****P* value < 0.001. (*B* and *C*) mRNA expressions were measured with primers targeting the common regions of E74.

of intermediate factors in the 20E-mediated repression. The transcript levels of the two EGs tested were high without 20E treatment but were significantly reduced in samples treated with 20E (Fig. 3*D* and *SI Appendix*, Fig. S4*D*). Addition of CHX to the 20E-containing culture medium compromised the 20E mediated repression of these genes (Fig. 3*D* and *SI Appendix*, Fig. S4*D*), indicating the involvement of intermediate downstream factors in their regulation.

Next, we performed an IVFBC experiment in tandem with RNAi depletion. Addition of 20E to the culture medium resulted in repression of the tested EGs, but the repressive effects were not observed in case of fat bodies with RNAi-depleted *E74* (Fig. 3*E* and *SI Appendix*, Fig. S4*E*), confirming that the repression of these target genes by 20E is indirect and through E74. Finally, we examined which of the two E74 isoforms was responsible for repressing these genes. *Aa*E74A transcript reportedly does not exhibit any significant increase until 24-h PBM and is elevated at 36-h PBM (25). Therefore, we hypothesized that *Aa*E74B, that shows a sharp elevation at 12- to 24-h PBM (25), is involved in the repression of EGs that are down-regulated during the same time period. We confirmed that the depletion of *Aa*E74A had no significant effect on the two E74 target EGs that were inhibited at 24-h PBM (Fig. 3*F* and *SI Appendix*, Fig. S4*F*). Finally, we confirmed the role of E74B by RNAi+IVFBC experiments where *E74B* was depleted with double-stranded RNA (dsRNA) specific to E74B. The repressive effects of 20E on the E74 target EGs could not be detected in samples with depleted E74B (Fig. 3*G* and *SI Appendix*, Fig. S4*G*). Taken together, these results demonstrated that in the presence of 20E, EcR activates *BR* expression that in turn activates *E74*. Finally, E74, specifically E74B, is responsible for the inhibition of the expression of its target genes.

Direct Repression of LMGs Occurs through a Specific Binding Motif for EcR and Utilizes Mi2 as a Corepressor.

20E and EcR are involved in the repression of LMGs. Seven cluster-specific overrepresented motifs were identified within the upstream regions of LMGs (Fig. 1). One of these motifs, TTGATTGA, is present within 53 CRRs of the 199 transcripts screened. TTGATTGA was suggested by JASPAR to be a putative target for EcR:USP. We examined whether this motif is an authentic target for EcR and whether USP, the heterodimeric partner of EcR within the ecdysone activation pathway, is involved in the repression of the downstream target genes.

We selected two LMGs that have the TTGATTGA motif within 1-kb upstream regions: *AAEL002658* (*amp dependent ligase*; motif 998 bases upstream of the translation start site), and *AAEL012037* (*sulfate transporter*; motif 242 bases upstream of the translation start site). As in the case of the EGs, the differential expression and the similarity of their expression profiles to that of the average expression profile of the LMGs, were used as the criteria for the selection of these two genes (*SI Appendix*, Fig. S3*B*). First, we tested the effects of iEcR on these genes by qRT-PCR. Transcripts for both the genes showed a significant increase (Fig. 4*A* and *SI Appendix*, Fig. S5*A*) when compared to the control iLuc, confirming that they are down-regulated by EcR in the FB at 24-h PBM. Next, we utilized CHX in the IVFBC system to test the necessity of intermediate factors in the 20E-mediated repression of these genes. The transcript levels of the two genes tested were high without 20E treatment but were significantly reduced in the samples treated with 20E (Fig. 4*B* and *SI Appendix*, Fig. S5*B*). Addition of CHX to the 20E-containing culture medium did not compromise their 20E-mediated repression (Fig. 4*B* and *SI Appendix*, Fig. S5*B*), suggesting that the repression of LMGs is direct and may require the TTGATTGA binding site for the binding of EcR to the CRRs of these genes. Thus, we examined the potential binding between EcR and the motif TTGATTGA. There are two known isoforms of EcR in mosquitoes, EcR-A and EcR-B (28). The transcripts of these isoforms exhibit dramatically different patterns of expression and are different in their sensitivity to 20E, after a blood meal-triggered activation of vitellogenesis in the FB (28). While EcR-A transcript levels peak at 16- to 20-h PBM coinciding with the 20E peak, EcR-B transcripts are at their lowest level at 16- to 24-h PBM (28). Therefore, to understand the role of EcR in direct repression of its target genes we have utilized EcR-A for all our subsequent molecular analyses.

EcR-A protein interacts with the specific EcREr in the promoters of LMGs. To confirm DNA–protein interaction, we performed ChIP assays in the cell culture system, using *Drosophila* S2 cells.

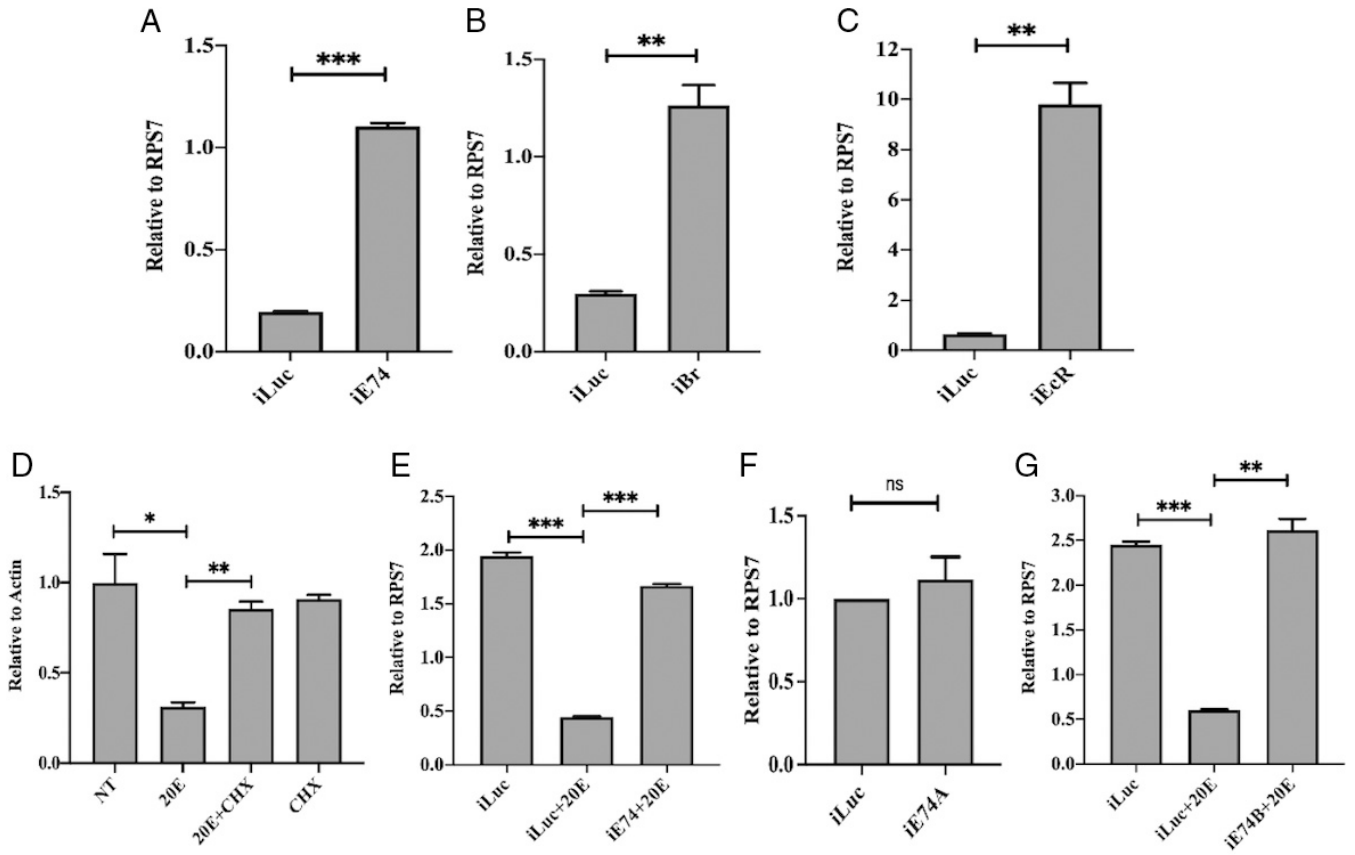

Fig. 3. Indirect repression of the target gene *Sideroflexin-1* (*AAEL014526*) by 20E through EcR, Br, and E74: (*A*–*C*) RNAi depletion of E74 (*A*), BR (*B*), and EcR (*C*) results in the up-regulation of the AAEL014526 transcript, indicating a down-regulation of the transcript by 20E through EcR, Br, and E74. All relative expressions were calculated against housekeeping gene RPS7. Injecting dsRNA for the *Luciferase* gene (iLuc) served as a control for all RNAi experiments. (*D*) Addition of CHX compromised the 20E-mediated repression of target gene *AAEL014526* indicating the necessity of protein synthesis for the process. *Actin* was used as the housekeeping gene. (*E*) Relative expression of AAEL014526 in tissues subjected to IVFBC in the culture media supplemented with amino acids, without (iLuc) and with 20E (iLuc+20E), showed a down-regulation of the AAEL014526 transcript with the addition of 20E. RNAi Depletion of the *E74* gene resulted in a rescue of the repressive effects of 20E on the AAEL014526 transcript. (*F*) RNAi depletion of *E74A* isoform had no significant effect on the AAEL014526 transcript indicating that E74A had no role in the down-regulation of this transcript. (*G*) Relative expression of AAEL014526 in tissues subjected to IVFBC in the culture media supplemented with amino acids, without (iLuc) and with 20E (iLuc+20E), showed a down-regulation of the AAEL014526 transcript with the addition of 20E. RNAi Depletion of the *E74B* isoform resulted in a rescue of the repressive effects of 20E on the AAEL014526 transcript. (*E*–*G*) Relative expressions were calculated against housekeeping gene RPS7. (*A*–*G*) Data are representative of three biological replicates, with three technical replicates and are illustrated as average ± SD, $*P < 0.05$; $**P < 0.01$; $***P < 0.001$. Injecting dsRNA for the *Luciferase* gene (iLuc) served as the control.

Myc-tagged full-length *Aedes* EcR-A (EcRA-Myc) was cloned in pAc5.1 vector (Invitrogen) and overexpressed in S2 cells. The endogenous *Dm*EcR was knocked down by RNAi. The CRRs of two LMGs *AAEL012037* and *AAEL002658*, harboring the putative EcREr element were cloned ($AAEL012037_{1Kb}$-Luc and $AAEL002658_{1Kb}$-Luc, respectively) and transfected into S2 cells treated with 10^{-6} M 20E, along with EcRA-Myc. Immunoprecipitations (IPs) were performed with anti-EcR antibody (DSHB), while anti-IgG antibody (Sigma) was used as mock control. Quantifications were performed by qRT-PCR using primer pairs targeting the EcREr region, while primers targeting plasmid backbone were used as control. A clear enrichment of EcREr region was observed in ChIP assays using anti-EcR antibody (Fig. 4*C* and *SI Appendix*, Fig. S6*A*) only in the presense of 20E (Fig. 4*D* and *SI Appendix*, Fig. S6*B*). These results confirmed the physical binding of EcR-A and the EcREr site in the target gene promoters.

The results were further confirmed by the EMSA. Coding regions for *Ae. aegypti* EcR-A and that of its heterodimeric partner USP-B were cloned into the pAc5.1-V5 vector (Invitrogen). *Drosophila* S2 cells were transfected with EcR-A and USP-B; 20E was added to the culture medium, followed by preparation of nuclear protein extracts from S2 cells. EMSAs were done and binding was detected (*SI Appendix*, Fig. S6*C*) with a labeled probe (synthesized oligos for site TTGATTGA and its flanking regions from the promoter of the EcR target gene *AAEL02658*) and nuclear protein extracts from S2 cells. Binding appeared to be specific based on comparison with 30× and 100× unlabeled specific (same sequence as the labeled probe) competitors (*SI Appendix*, Fig. S6*C*), as increasing the amounts of the unlabeled probe reduced the binding of the labeled probe. Addition of *Drosophila* EcR antibody resulted in the disappearance of the specific band (*SI Appendix*, Fig. S6*C*). Addition of *Drosophila* anti-USP antibody had no effect on the binding; however, when both antibodies (anti-EcR and anti-USP) were added the band disappeared (*SI Appendix*, Fig. S6*C*). The disappearance of the specific band with addition of anti-EcR antibody with or without anti-USP suggested that *Aedes* USP may not have a role in 20E/EcR-mediated repression of target genes. Finally, we used two labeled probes with mutated EcREr (*SI Appendix*, Table S3); no band was detected for these probes (*SI Appendix*, Fig. S6*D*) confirming the binding specificity of the EcREr.

Corepressor* Aa*Mi2, but not* Aa*USP, is involved in 20E/EcR–mediated gene repression. To confirm the role of USP, we designed dsRNA targeting *USP-A*, *USP-B*, or *USP* core regions (*USP-core*). Depletion of either *USP-A* or *USP-B* or *USP-core* did not alter the expression of the target genes, *AAEL002658* and

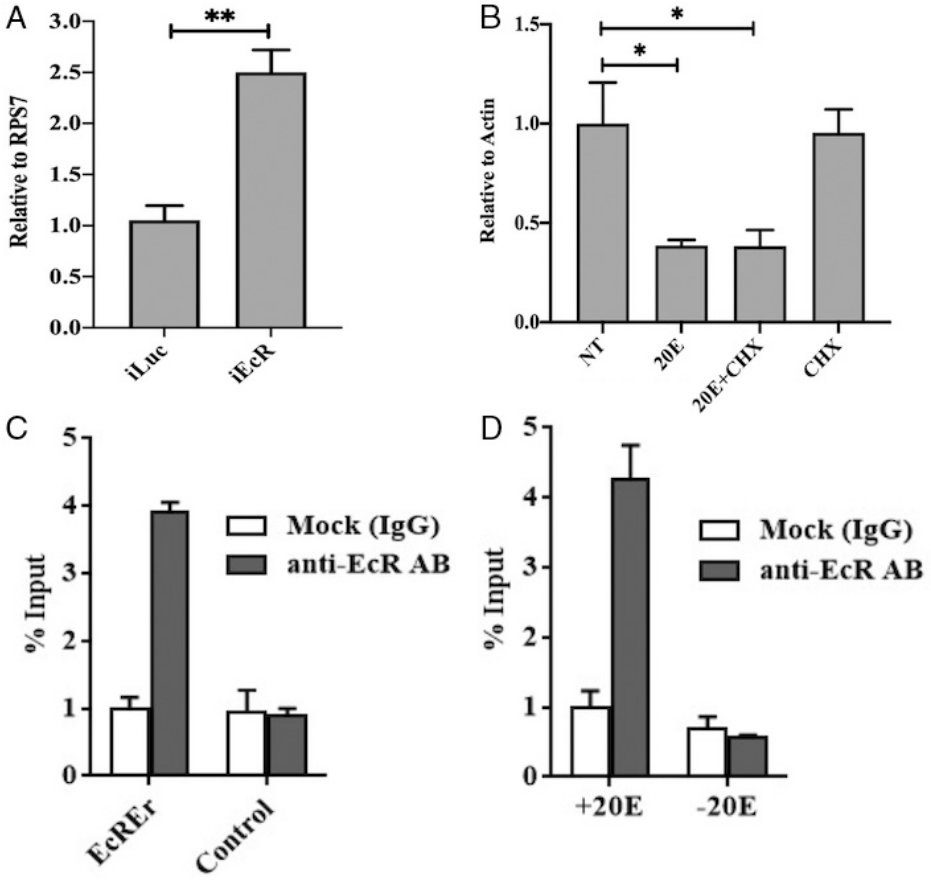

Fig. 4. Direct repression of the 20E/EcR target gene *Sulfate transporter* (*AAEL012037*) by EcR: (*A*) RNAi depletion of EcR results in up-regulation of the AAEL012037 transcript, indicating a down-regulation of the transcript by 20E through EcR. Relative expression detected by qRT-PCR, in FB tissues collected from iEcR female mosquitoes. iLuc served as a control and *RPS7* was used as the housekeeping gene. (*B*) Addition of CHX does not compromise the 20E-mediated repression of target gene *AAEL012037*, indicating that protein synthesis is not required for the process. *Actin* was used as the housekeeping gene. (*A* and *B*) Data are representative of three biological replicates, with three technical replicates and are illustrated as average ± SD, $*P < 0.05$; $**P < 0.01$. (*C* and *D*) EcR-A interacts with a unique EcREr (TTGATTGA motif): Cell culture-based ChIP assays demonstrating the binding of EcR-A protein to specific EcREr DNA elements (*C*) in the CRR of target gene *AAEL012037* (*D*) only in the presence of 20E. AAEL012037$_{1Kb}$-Luc and EcRA-Myc was transfected into S2 cells. ChIPs were performed with anti-EcR antibody. Anti-IgG antibody was used as mock control. Data were represented as % of input DNA. Error bars represent ± SD.

AAEL012037 (*SI Appendix*, Fig. S7), when compared to the control iLuc, suggesting that USP does not participate in the repression of these genes by EcR in the presence of 20E.

To search for additional factors involved in 20E/EcR repression, we performed RNAi of cofactors previously implicated in *Drosophila* ecdysone pathway. Specifically, we performed RNAi for *Aedes* ortholog of *Smrter* (XP_021708961.1), *Alien* (AAEL005730), *Mi2* (AAEL027786), and *Hormone Receptor 38* (HR38; AAEL022402), followed by blood feeding and gene-expression analysis by qRT-PCR. iLuc was used as a negative control, while iEcR served as the positive control. Only *Mi2* knockdown (iMi2) phenocopied the effect of *EcR* depletion on the expression of LMGs, *AAEL012037* and *AAEL002658* (Fig. 5*A* and *SI Appendix*, Fig. S8*A*), indicating that Mi2 may act in the 20E/EcR gene repression pathway. To further access the role of *Aa*Mi2 we performed IVFBC experiments with iLuc, iEcR, or iMi2 mosquitoes with and without 20E (10^{-6} M). Repression of the target genes were observed in 20E treated iLuc mosquitoes in comparison to nontreated controls (Fig. 5*B* and *SI Appendix*, Fig. S8*B*). 20E repressive action was compromised in iEcR mosquitoes indicating that the signal works through EcR. Like iEcR, RNAi of *Aa*Mi2 rendered the system nonfunctional to 20E action, indicating that a functional *Aa*Mi2 is necessary for 20E/EcR mediated gene repression (Fig. 5*B* and *SI Appendix*, Fig. S8*B*).

***Aa*Mi2 is a component of 20E/EcR complex that binds to the EcREr element.** Next, we examined whether EcR and *Aa*Mi2 physically interact with each other by conducting coimmunoprecipitation experiments (co-IP). Flag-tagged full-length *Aa*Mi2 (Mi2-Flag) were cloned in pAc5.1. Both EcRA-Myc and Mi2-Flag were transfected into S2 cells. The culture medium was supplemented with dsRNA targeting *Dm*EcR and *Dm*Mi2 and the cells were treated with 10^{-6} M 20E. After IP with anti-EcR antibody, Mi2-Flag was detected in Western blots (WBs) with anti-Flag antibody only when both fusion proteins were coexpressed in the cell culture system (Fig. 5*C*). The protein–protein interaction between *Aedes* EcR and *Aa*Mi2 were further confirmed by additional co-IP experiments (IP:anti-Myc, WB:anti-Flag; IP:anti-Flag, WB:anti-Myc; IP:anti-Flag, WB:anti-EcR), where a band was detected only when both proteins were present (Fig. 5*C*).

To determine if *Aa*Mi2 protein associates with the EcREr motif in CRRs of target genes repressed by 20E/EcR action, we conducted culture-based ChIP assays. The AAEL012037$_{1Kb}$-Luc and AAEL002658$_{1Kb}$-Luc plasmids harboring EcREr motif was transfected into S2 cells along with EcRA-Myc and Mi2-Flag. Endogenous factors, *Dm*EcR and *Dm*Mi2 were depleted via RNAi. The cells were then treated with 20E (10^{-6} M). Since Mi2 is known to function as corepressor that does not directly bind to the primary TF recognition site (29), we utilized a dual cross-linking protocol as described in *SI Appendix*, *Materials and Methods*.

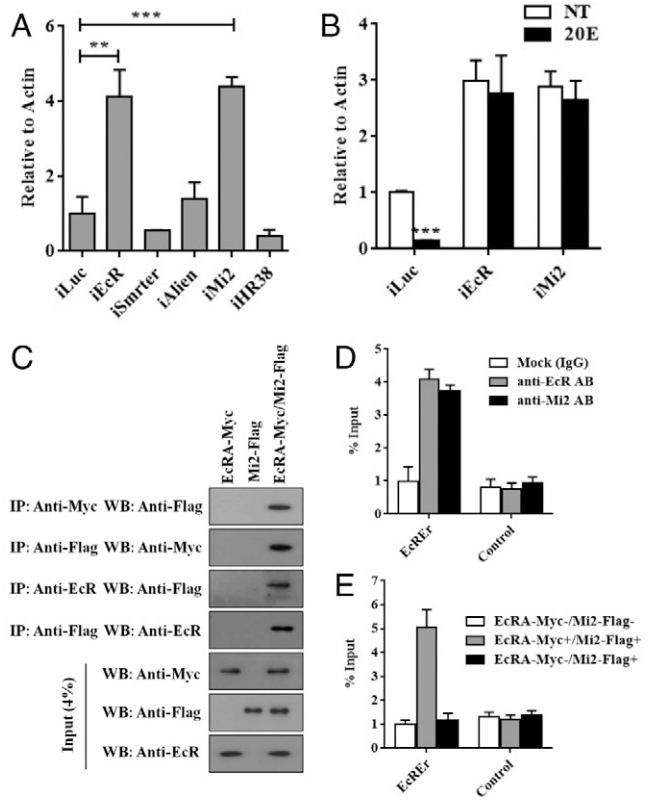

Fig. 5. *Aa*Mi2 is involved in the 20E/EcR gene repression pathway. (*A*) dsRNA-mediated depletion of *Aa*Mi2 phenocopies the effect of EcR knockdown on the expression target gene *AAEL012037*. Knockdown of other tested factors—*Aa*Smrter, *Aa*Alien, *Aa*Hr38—did not impact the expression of target gene. (*B*) IVFBC experiments demonstrating effects of 20E on the expression of AAEL012037 in iLuc, iEcR, and iMi2 samples. 20E mediated repression of the target gene was compromised in both iEcR and iMi2 mosquitoes. (*A* and *B*) iLuc was used as control. All experiments were performed in triplicates with similar results. Error bars represent ± SD ***P* value < 0.01, ****P* value < 0.001. (*C*) Co-IP experiments showing protein–protein interaction between *Aedes* EcR and *Aa*Mi2. EcRA-Myc and Mi2-Flag was overexpressed in S2 cells either independently or together. Endogenous *Dm*EcR and *Dm*Mi2 were knocked down using dsRNA. (*D*) ChIP assays demonstrating the association of *Aa*Mi2 with EcREr in the promoter region of 20E/EcR target gene *AAEL012037*. AAEL012037$_{1Kb}$-Luc was transected into S2 cells along with EcRA-Myc and Mi2-Flag. IPs were performed with *Drosophila* anti-EcR and anti-Mi2 antibody. anti-IgG antibody was used as mock control. (*E*) ChIP assays performed with AAEL012037$_{1Kb}$-Luc and either both EcRA-Myc and Mi2-Flag (EcRA-Myc^{+}/Mi2-Flag^{+}) or Mi2-Flag only (EcRA-Myc^{-}/Mi2-Flag^{-}), demonstrating the need for functional EcR-A protein for the association of Mi2 with EcREr elements. Cells devoid of both EcRA-Myc and Mi2-Flag (EcRA-Myc^{-}/Mi2-Flag^{-}) were used as controls. IPs were performed with commercially available anti-Flag antibodies. (*D* and *E*) Endogenous *Dm*EcR and *Dm*Mi2 were knocked down using dsRNA. Data were represented as percent of input DNA. Error bars represent ±SD.

IPs were performed using antibodies against *Drosophila* EcR and Mi2. A clear enrichment in signal was observed with ChIP assays using anti-Mi2 antibody, phenocopying the results from anti-EcR antibody-based ChIPs (Fig. 5*D* and *SI Appendix*, Fig. S9*A*). These results indicate an association between Mi2 and EcREr in the presence of EcR and 20E.

To investigate whether the presence of EcR is a prerequisite for the association between *Aa*Mi2 and EcREr, we performed ChIP assays in S2 cells transfected with expression vector EcRA-Myc and Mi2-Flag in the following combinations: EcRA-Myc^{+}/Mi2-Flag^{+} and EcRA-Myc^{-}/Mi2-Flag^{+}. Cells devoid of both EcR-Myc and Mi2-Flag (EcRA-Myc^{-}/Mi2-Flag^{-}) were used as controls. Both AAEL012037$_{1Kb}$-Luc and AAEL002658$_{1Kb}$-Luc were tested and IPs were performed with anti-Flag antibody. A signal was detected for EcREr when both factors were present in the system (Fig. 5*E* and *SI Appendix*, Fig. S9*B*). However, no enrichment was observed when only Mi2-Flag was expressed, indicating that its association with EcREr requires EcR protein (Fig. 5*E* and *SI Appendix*, Fig. S9*B*). Thus, our experiments suggest that the ligand bound EcR binds EcREr, recruiting *Aa*Mi2 as a corepressor.

Luciferase reporter assays demonstrated the direct repression of target LMGs by the 20E/EcR/Mi2 complex. We have identified a previously unreported EcREr element, demonstrated its physical interaction with *Aa*EcR, and identified *Aa*Mi2 as a putative cofactor of 20E/EcR-mediated gene repression. To test our model, we performed luciferase reporter assays using S2 cells. Expression vectors EcRA-Myc and Mi2-Flag and reporter vectors AAEL012037$_{1Kb}$-Luc and AAEL002658$_{1Kb}$-Luc were used for this purpose. First, a titration with 10^{-8}, 10^{-7}, 10^{-6}, and 10^{-5} M 20E was performed on cells transfected with AAEL012037$_{1Kb}$-Luc. A clear repression in luciferase activity was observed with increasing concentration of 20E, which peaked at 10^{-6} M reaching saturation beyond this dosage (*SI Appendix*, Fig. S10*A*). To test the effect of *Aa*EcR, S2 cells were transfected with AAEL012037$_{1Kb}$-Luc and increasing concentrations of EcRA-Myc (50, 100, 200, and 400 ng), followed by 20E treatment (10^{-6} M). The endogenous *Dm*EcR was knocked down by RNAi. Significant repression of luciferase activity was observed, and the signal was reduced to almost background levels when 200 ng of EcRA-Myc was transfected into the cell line (*SI Appendix*, Fig. S10*B*).

Next, we investigated the role of the EcREr motif 5′-TTGATTGA-3′ on gene repression. A construct was generated by mutating EcREr motif to 5′-CATATG-3′, and leaving the rest of the plasmid intact (AAEL012037$_{1Kb}$ΔEcRE-Luc). EcRA-Myc, AAEL012037$_{1Kb}$-Luc, and AAEL012037$_{1Kb}$ΔECRE-Luc were variously transfected into the S2 cells followed by hormonal treatment, when required. All cells were treated with dsRNA targeting endogenous *Dm*EcR. Expectedly, a substantial reduction in luciferase signal was recorded when 20E, EcRA-Myc, and AAEL012037$_{1Kb}$-Luc were present in the system (Fig. 6*A*). However, the repression was compromised when cells were transfected with the mutant vector AAEL012037$_{1Kb}$ΔEcREr-Luc (Fig. 6*B*) instead, indicating that the repressive signal is transmitted via binding of EcR-A to EcREr motif (Fig. 6*A*). Similar experiments were performed with the second gene promoter AAEL002658$_{1Kb}$-Luc and its mutant AAEL002658$_{1Kb}$ΔEcREr-Luc (where the EcREr site was changed to 5′-CTCGAG-3′) (*SI Appendix*, Fig. S11 *A* and *B*). The mutation resulted in a loss of repressive action of 20E/EcR, providing support for our hypothesis (*SI Appendix*, Fig. S11*A*).

Thereafter, we explored the role of the third component, the cofactor *Aa*Mi2. We anticipated that endogenous *Dm*Mi2 protein is responsible for the success of the above experiments. Indeed, RNAi for *Dm*Mi2 in cell culture system mentioned above completely compromised the 20E-mediated gene repression (Fig. 6*C* and *SI Appendix*, Fig. S11*C*). The repressive action of 20E/EcR was restored by overexpression of *Aa*Mi2 protein in the system (Fig. 6*C* and *SI Appendix*, Fig. S11*C*). All cells were treated with dsRNA for *Dm*EcR. The expression of tagged proteins EcRA-Myc and Mi2-Flag in S2 cells were validated by anti-Myc and anti-Flag antibodies, respectively (*SI Appendix*, Fig. S10*C*). The efficacy of RNAi knockdowns of *Dm*EcR and *Dm*Mi2 in S2 cells was confirmed by Western blots (*SI Appendix*, Fig. S10*D*).

20E/EcR/Mi2 action leads to chromatin-mediated compaction of the target gene locus. We next asked whether the receptor complex for 20E direct repression modulates the chromatin

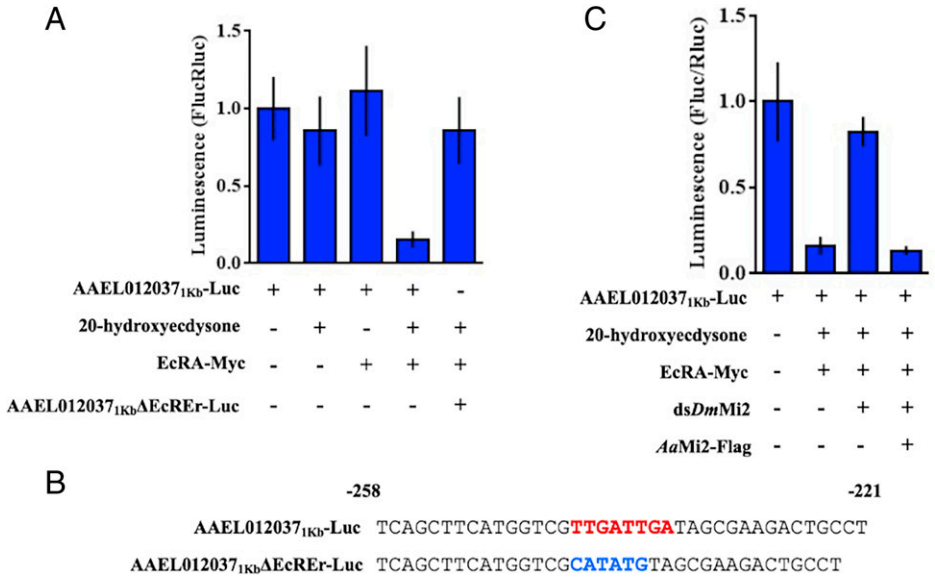

Fig. 6. Functional analysis of 20E/EcR/Mi2 repressor complex. (*A*) Luciferase reporter assays demonstrating direct repression by 20E/EcR through target gene CRR harboring EcREr. S2 cells were cotransfected with expression vector EcRA-Myc and reporter plasmid AAEL012037$_{1Kb}$-Luc, along with 20E supplementation of culture medium when required. Reporter plasmid with a mutated EcREr (AAEL012037$_{1Kb}$ΔEcREr-Luc) was also used to demonstrate the necessity of the DNA element in transrepression of reporter gene. (*B*) The putative EcR binding site along with flanking regions harbored within 1-kb region of *AAEL012037* gene promoter and the mutated sequences utilized in this experiment are indicated. (*C*) Luciferase reporter assay demonstrating the necessity of a functional Mi2 protein for 20E/EcR mediated repression of target gene *AAEL012037*. RNAi depletion of endogenous *Dm*Mi2 results in compromised repression via 20E/EcR. The phenotype could be rescued by overexpression of Mi2-Flag in the system. (*A–C*) *Dm*EcR was knocked down via RNAi in all samples. Error bars represent ± SD.

structure of the target gene *AAEL012037*. To address this question, we performed micrococcal nuclease (MNase) digestion of chromatin followed by qRT-PCR–based quantification of the relative MNase protection of target gene regions, in iEcR and iMi2 mosquitoes. Protection from MNase digestion suggests greater chromatin compaction and results in higher qRT-PCR product levels. Primers targeting five loci in the gene *AAEL012037* (A, B, and C targeting the promoter region; D and E targeting exon regions) were utilized to quantitate relative MNase protection (Fig. 7, *Upper*). Of these, region C harbors both the EcREr element as well as the TSS (Fig. 7, *Upper*). *Mi2* RNAi resulted in clear susceptibility to MNase digestion indicating a reduction in chromatin compaction at the *AAEL012037* CRR (at loci A, B, and C) in the FB, 24-h PBM (Fig. 7, *Lower*). However, RNAi of *Mi2* did not affect the MNase digestion profile of assayed exon regions, D and E, of *AAEL012037* (Fig. 7, *Lower*). RNAi of *EcR* provides similar results as the iMi2 samples, emphasizing the necessity of EcR-mediated recruitment of Mi2 in target gene loci to initiate chromatin compaction (Fig. 7, *Lower*).

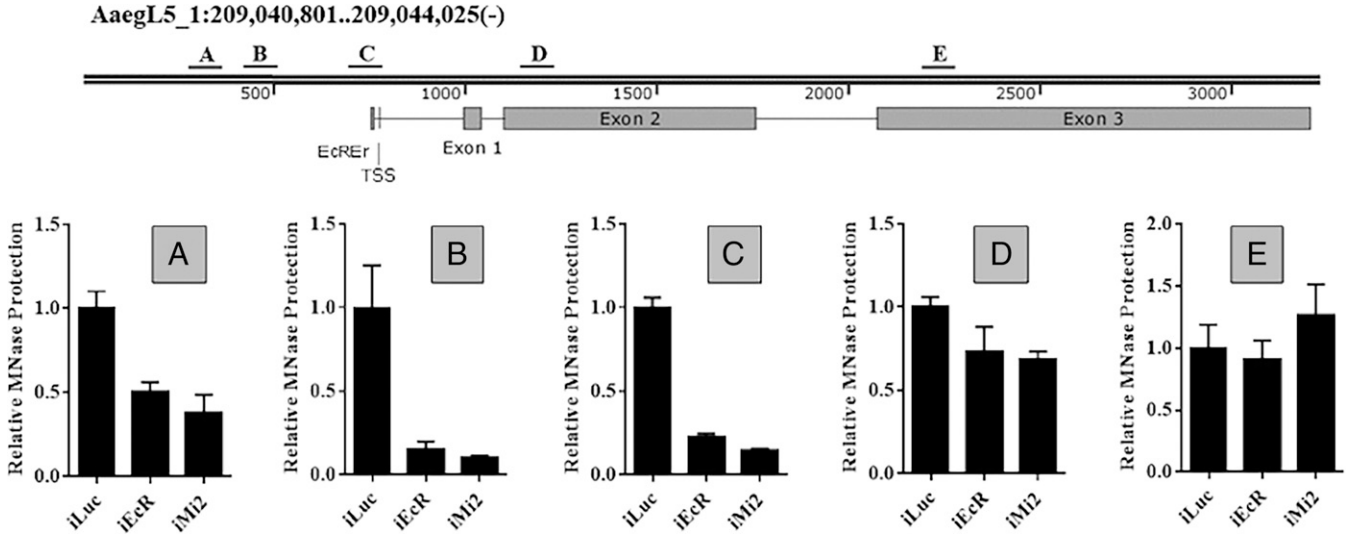

Fig. 7. MNase protection assay demonstrating the effect of EcR/Mi2 in chromatin compaction of target gene *AAEL012037*. (*Upper*) Schematic representation of target region amplifications within the *AAEL012037* gene locus. Loci A to C target the promoter region, while loci D and E target exonic regions within the gene. (*Lower*) Preblood-fed mosquitoes were treated with dsRNA for either EcR or Mi2, followed by blood feeding and FB collection. iLuc was used as controls. Chromatin was prepared from the tissue samples and was subjected to MNase digestion. Quantification for relative MNase protection was performed by qRT-PCR using primers targeting A to E loci of gene *AAEL012037*. Undigested chromatin was used as internal control. Error bars represent ±SD. All experiments were performed in triplicates with similar results.

Discussion

CREs Identified in This Study Provide Insights into Multiple Regulatory Pathways in Mosquito Reproduction. The event of TFs binding to their corresponding binding sites is one of the primary biological processes determining gene expression. In silico prediction of TFBSs followed by functional assessment through molecular biology methods can lead to accurate assessment of CRRs. In this study, the use of two different algorithm-based motif prediction programs have increased the accuracy and reliability of the detected overrepresented motifs. All overrepresented motifs may not be TFBSs; therefore, we employed three different bioinformatics tests, related to the characteristics of real TFBSs. In addition to checking for positional and orientation bias, we also checked for evolutionary conservation using the sequences from two other mosquito species that have been sequenced and annotated. The reason behind checking evolutionary conservation is motivated by the fact that regulation mechanisms and binding sites are preserved in an appropriate evolutionary distance except for inordinate background conservation (30).

The JASPAR database provided us with a list of putative TFs that could bind to a specific motif. In principle, the multistep approach used here for identifying the putative TFBSs should yield good initial results; it is still possible that some of the predicted candidate motifs may be false positives. It is also possible that real TFBSs, if they are not overrepresented, might be undetected. Despite these two drawbacks of the computational motif discovery scheme, we believe that the results, in general, from the suggested approach are reliable. We did observe that the annotations for the TSSs in "Vectorbase" were not always accurate; to counter this problem, we have used 2-kb upstream CRRs (31). Along with providing an insight into the regulatory mechanism of genes, the CREs may have significant practical applications. These can be used to generate transgenic mosquitoes, refractory to disease transmission, for vector control strategies like population suppression or replacement (32–34).

Gene Regulatory Networks Provide an Insight into Direct and Indirect Negative Regulation of Transcripts by the Ecdysone Regulatory Cascade. The prevailing model for 20E action suggests that the EcR-USP heterodimer activates the expression of genes in the presence of 20E (35), and in the absence of hormone, EcR-USP is known to repress target gene activity (36–38). Conversely, several genes have been shown to be down-regulated as a result of 20E/EcR action in *Drosophila melanogaster* and *Ae. aegypti* (4, 26, 39, 40). However, the mechanism of repression by the ligand-bound EcR remained largely unexplored, particularly in mosquitoes. We investigated the molecular mechanism of 20E/EcR-mediated gene repression in *Ae. aegypti* and have demonstrated that 20E-liganded EcR binds directly to the EcREr (TTGATTGA) identified in the CRRs of some LMGs in order to negatively regulate their expression. ChIP and EMSA assays have proven that EcR-A recognizes the specific TTGATTGA site. EcR:USP binding sites that include inverted repeat of TTGA (5′-CGTTGAAT CAATG-3′) and that with TTGA half sites (5′-GGTTGAAT GAATT-3′, 5′-ATTTCTTTGAATT-3′) have been reported (40). However, in this study we have shown that a direct repeat of the TTGA site without any spacers is recognized by EcR-A. We have also demonstrated that the canonical EcR binding partner USP is not involved in 20E/EcR-mediated gene repression in the mosquito. Recent ChIP-sequencing studies in *Drosophila* have also identified many EcR-associated genomic regions devoid of USP (29, 41). This suggests that specific DNA motifs facilitate the recruitment of EcR in the presence of 20E in *Drosophila.* Whether liganded EcR binds DNA as a monomer or a homodimer requires further investigation. Also, the mutation of the EcREr site in a luciferase reporter assay resulted in the loss of the reporter gene repression, adding further evidence to this hypothesis. We performed ChIP and luciferase assays to confirm that EcRB does not recognize EcREr in the presence of 20E, and therefore has no role in direct repression of target LGs (*SI Appendix*, Fig. S12).

Here we have demonstrated that in the mosquito *Ae. aegypti*, Mi2 acts as a corepressor in the 20E/EcR-mediated gene repression. Insect Mi2 proteins are homologs of the widely conserved CHD family of ATP-dependent nucleosome remodelers. Mi2 protein is an integral component of a large macromolecular complex called Mi2/nucleosome remodeling and deacetylase (NuRD) that are known to regulate various developmental processes (42, 43). The Mi2/NuRD complex has been reported to be abundantly present in various organisms with a broad cellular and tissue distribution (44–46). The complex is known to cooperate with various TFs in establishing specific transcription programs that generate the chromatin environment appropriate for gene repression (47, 48). Our MNase protection assays indicate that Mi2, recruited by 20E-liganded EcR to CRRs of 20E-repressed genes, constraining target gene transcription by inducing chromatin compaction. Similarly, *Drosophila* Mi2 has been shown to induce chromatin compaction of genes like *Broad* and *Vrille* in the presence of 20E (29). This study by Krehrer et al. (29) and our findings provide primary evidence concerning the direct role of 20E in inducing chromatin compaction at a target gene locus.

On the other hand, most EGs, that are also down-regulated at the high titer of 20E, lack the EcREr. Our results suggest that 20R/EcR activates BR, a canonical ecdysone target gene, that in turn activates E74. During *Drosophila* development, prior expression of BR proteins is required for the induction of the early primary-response genes and the EcR protein complex by itself is not sufficient for the activation (22). E74B, one of the E74 isoforms has been shown to be involved in repression of downstream genes in the ecdysone regulatory cascade (49). Therefore, our results, which show that E74 is involved in the repression of certain target genes, are congruent with the above-mentioned reports. However, the mechanism of repression by E74 isoforms requires further investigation.

In conclusion, we have characterized two negative regulatory pathways for the liganded EcR regulatory cascade during 20E-driven reproduction of the female *Ae. aegypti.* Genes within the two groups (EGs and LMGs) that have distinctly different expression profiles but both exhibit low levels of expression at the high titer of 20E, are negatively regulated by the 20E/EcR cascade by distinctly different molecular mechanisms. In the case of EGs, E74 is activated by the 20E-liganded EcR through BR, and in turn is responsible for repression of EGs. In contrast, LMGs are repressed directly by EcR that recognizes a previously unreported EcREr within their CRRs recruiting Mi2 that acts as a corepressor initiating chromatin condensation at LMG loci.

Materials and Methods

A detailed description of the materials and methods is given in *SI Appendix, Materials and Methods*. In brief, the culture of *Ae. aegypti* mosquitoes, RNAi, qRT-PCR, and IVFBC were performed according to the previously described protocols (4). EMSA, ChIP assays, and luciferase reporter assays were performed according to Saha et al. (27).

Data Availability. All study data are included in the article and/or *SI Appendix*.

ACKNOWLEDGMENTS. We thank Dr. Naoki Yamanaka (University of California, Riverside, CA) for critical reading of the manuscript and helpful suggestions. Portions of this paper were part of J.H.'s dissertation, "Identification of *cis*-regulatory elements and miRNA targets involved in mosquito reproduction." This work was supported by NIH Grant R01 AI036959 (to S.R. and A.S.R.), a start-up grant from the University of Texas El Paso (to S.R.), Department of Science and Technology-Science and Engineering Research Board Grant SRG/2019/000730 (to T.T.S.), and Start-up Grant GOA/ACG/2019-20/Oct/07 from Bits Goa (to T.T.S.).

Author affiliations: [a]Department of Entomology, University of California, Riverside, CA 92521; [b]Department of Biological Sciences, University of Texas at El Paso, El Paso, TX 79968; [c]Department of Biological Sciences, Birla Institute of Technology and Sciences, K. K. Birla Goa Campus, 403726 Goa, India; and [d]Graduate Program in Genetics, Genomics, and Bioinformatics, University of California, Riverside, CA 92521

1. A. D. T. Barrett, S. Higgs, Yellow fever: A disease that has yet to be conquered. *Annu. Rev. Entomol.* **52**, 209–229 (2007).
2. E. Calvez *et al.*, Genetic diversity and phylogeny of *Aedes aegypti*, the main arbovirus vector in the Pacific. *PLoS Negl. Trop. Dis.* **10**, e0004374 (2016).
3. S. B. Halstead, Dengue virus-mosquito interactions. *Annu. Rev. Entomol.* **53**, 273–291 (2008).
4. S. Roy *et al.*, Regulation of gene expression patterns in mosquito reproduction. *PLoS Genet.* **11**, e1005450 (2015).
5. N. Yamanaka, K. F. Rewitz, M. B. O'Connor, Ecdysone control of developmental transitions: Lessons from Drosophila research. *Annu. Rev. Entomol.* **58**, 497–516 (2013).
6. A. S. Raikhel, M. R. Brown, X. Belles, Hormonal control of reproductive processes. *Compre. Mol. Insect Sci.* **3**, 433–491 (2005).
7. S. Roy *et al.*, Chapter five: Regulation of reproductive processes in female mosquitoes *Adv. Insect Physiol.***51**, 115–144 (2019).
8. C. M. Uyehara, D. J. McKay, Direct and widespread role for the nuclear receptor EcR in mediating the response to ecdysone in *Drosophila*. *Proc. Natl. Acad. Sci. U.S.A.* **116**, 9893–9902 (2019).
9. E. T. Danielsen *et al.*, A Drosophila genome-wide screen identifies regulators of steroid hormone production and developmental timing. *Dev. Cell* **37**, 558–570 (2016).
10. M. Shibata, F. O. Gulden, N. Sestan, From *trans* to *cis*: Transcriptional regulatory networks in neocortical development. *Trends Genet.* **31**, 77–87 (2015).
11. L. W. Barrett, S. Fletcher, S. D. Wilton, Regulation of eukaryotic gene expression by the untranslated gene regions and other non-coding elements. *Cell. Mol. Life Sci.* **69**, 3613–3634 (2012).
12. S. H. Ji, "Identification of *cis*-regulatory elements and miRNA targets involved in mosquito reproduction," PhD thesis, University of California, Riverside, CA (2016).
13. T. L. Bailey *et al.*, MEME SUITE: Tools for motif discovery and searching. *Nucleic Acids Res.* **37**, W202–W208 (2009).
14. G. Pavesi, P. Mereghetti, G. Mauri, G. Pesole, Weeder Web: Discovery of transcription factor binding sites in a set of sequences from co-regulated genes. *Nucleic Acids Res.* **32**, W199–W203 (2004).
15. O. Elemento, N. Slonim, S. Tavazoie, A universal framework for regulatory element discovery across all genomes and data types. *Mol. Cell* **28**, 337–350 (2007).
16. R. Janky, J. van Helden, Evaluation of phylogenetic footprint discovery for predicting bacterial *cis*-regulatory elements and revealing their evolution. *BMC Bioinformatics* **9**, 37 (2008).
17. R. C. Hardison, Conserved noncoding sequences are reliable guides to regulatory elements. *Trends Genet.* **16**, 369–372 (2000).
18. R. C. Edgar, MUSCLE: Multiple sequence alignment with high accuracy and high throughput. *Nucleic Acids Res.* **32**, 1792–1797 (2004).
19. S. Gupta, J. A. Stamatoyannopoulos, T. L. Bailey, W. S. Noble, Quantifying similarity between motifs. *Genome Biol.* **8**, R24 (2007).
20. V. R. Chintapalli, J. Wang, J. A. T. Dow, Using FlyAtlas to identify better *Drosophila melanogaster* models of human disease. *Nat. Genet.* **39**, 715–720 (2007).
21. D. Warde-Farley *et al.*, The GeneMANIA prediction server: Biological network integration for gene prioritization and predicting gene function. *Nucleic Acids Res.* **38**, W214–W220 (2010).
22. F. D. Karim, G. M. Guild, C. S. Thummel, The Drosophila Broad-Complex plays a key role in controlling ecdysone-regulated gene expression at the onset of metamorphosis. *Development* **118**, 977–988 (1993).
23. J. C. Fletcher, K. C. Burtis, D. S. Hogness, C. S. Thummel, The Drosophila E74 gene is required for metamorphosis and plays a role in the polytene chromosome puffing response to ecdysone. *Development* **121**, 1455–1465 (1995).
24. G. Sun, J. Zhu, L. Chen, A. S. Raikhel, Synergistic action of E74B and ecdysteroid receptor in activating a 20-hydroxyecdysone effector gene. *Proc. Natl. Acad. Sci. U.S.A.* **102**, 15506–15511 (2005).
25. G. Sun, J. Zhu, C. Li, Z. Tu, A. S. Raikhel, Two isoforms of the early E74 gene, an Ets transcription factor homologue, are implicated in the ecdysteroid hierarchy governing vitellogenesis of the mosquito, *Aedes aegypti*. *Mol. Cell. Endocrinol.* **190**, 147–157 (2002).
26. D. Shlyueva *et al.*, Hormone-responsive enhancer-activity maps reveal predictive motifs, indirect repression, and targeting of closed chromatin. *Mol. Cell* **54**, 180–192 (2014).
27. T. T. Saha *et al.*, Hairy and Groucho mediate the action of juvenile hormone receptor Methoprene-tolerant in gene repression. *Proc. Natl. Acad. Sci. U.S.A.* **113**, E735–E743 (2016).
28. S. F. Wang, C. Li, G. Sun, J. Zhu, A. S. Raikhel, Differential expression and regulation by 20-hydroxyecdysone of mosquito ecdysteroid receptor isoforms A and B. *Mol. Cell. Endocrinol.* **196**, 29–42 (2002).
29. J. Kreher *et al.*, EcR recruits dMi-2 and increases efficiency of dMi-2-mediated remodelling to constrain transcription of hormone-regulated genes. *Nat. Commun.* **8**, 14806 (2017).
30. S. Santini, J. L. Boore, A. Meyer, Evolutionary conservation of regulatory elements in vertebrate Hox gene clusters. *Genome Res.* **13**, 1111–1122 (2003).
31. M. Bonizzoni *et al.*, Complex modulation of the *Aedes aegypti* transcriptome in response to dengue virus infection. *PLoS One* **7**, e50512 (2012).
32. O. S. Akbari *et al.*, A synthetic gene drive system for local, reversible modification and suppression of insect populations. *Curr. Biol.* **23**, 671–677 (2013).
33. F. Catteruccia, A. Crisanti, E. A. Wimmer, Transgenic technologies to induce sterility. *Malar. J.* **8** (suppl. 2), S7 (2009).
34. L. Alphey, D. Nimmo, S. O'Connell, N. Alphey, "Insect population suppression using engineered insects" in *Transgenesis and the Management of Vector-Borne Disease*, S. Aksoy, Ed. (Springer New York, 2008), pp. 93–103.
35. R. J. Hill, I. M. L. Billas, F. Bonneton, L. D. Graham, M. C. Lawrence, Ecdysone receptors: From the Ashburner model to structural biology. *Annu. Rev. Entomol.* **58**, 251–271 (2013).
36. Y. Z. He, E. Aksoy, Y. Ding, A. S. Raikhel, Hormone-dependent activation and repression of microRNAs by the ecdysone receptor in the dengue vector mosquito *Aedes aegypti*. *Proc. Natl. Acad. Sci. U.S.A.* **118**, e2102417118 (2021).
37. L. Dobens, K. Rudolph, E. M. Berger, Ecdysterone regulatory elements function as both transcriptional activators and repressors. *Mol. Cell. Biol.* **11**, 1846–1853 (1991).
38. C. C. Tsai, H. Y. Kao, T. P. Yao, M. McKeown, R. M. Evans, SMRTER, a Drosophila nuclear receptor coregulator, reveals that EcR-mediated repression is critical for development. *Mol. Cell* **4**, 175–186 (1999).
39. R. B. Beckstead, G. Lam, C. S. Thummel, The genomic response to 20-hydroxyecdysone at the onset of *Drosophila metamorphosis*. *Genome Biol.* **6**, R99 (2005).
40. Z. Gauhar *et al.*, Genomic mapping of binding regions for the ecdysone receptor protein complex. *Genome Res.* **19**, 1006–1013 (2009).
41. D. Y. Rhee *et al.*, Transcription factor networks in *Drosophila melanogaster*. *Cell Rep.* **8**, 2031–2043 (2014).
42. P. S. Knoepfler, R. N. Eisenman, Sin meets NuRD and other tails of repression. *Cell* **99**, 447–450 (1999).
43. S. A. Denslow, P. A. Wade, The human Mi-2/NuRD complex and gene regulation. *Oncogene* **26**, 5433–5438 (2007).
44. T. von Zelewsky *et al.*, The *C. elegans* Mi-2 chromatin-remodelling proteins function in vulval cell fate determination. *Development* **127**, 5277–5284 (2000).
45. P. A. Wade, P. L. Jones, D. Vermaak, A. P. Wolffe, A multiple subunit Mi-2 histone deacetylase from *Xenopus laevis* cofractionates with an associated Snf2 superfamily ATPase. *Curr. Biol.* **8**, 843–846 (1998).
46. J. K. Tong, C. A. Hassig, G. R. Schnitzler, R. E. Kingston, S. L. Schreiber, Chromatin deacetylation by an ATP-dependent nucleosome remodelling complex. *Nature* **395**, 917–921 (1998).
47. B. A. Reddy *et al.*, Drosophila transcription factor Tramtrack69 binds MEP1 to recruit the chromatin remodeler NuRD. *Mol. Cell. Biol.* **30**, 5234–5244 (2010).
48. N. Kunert *et al.*, dMec: A novel Mi-2 chromatin remodelling complex involved in transcriptional repression. *EMBO J.* **28**, 533–544 (2009).
49. J. C. Fletcher, P. P. D'Avino, C. S. Thummel, A steroid-triggered switch in E74 transcription factor isoforms regulates the timing of secondary-response gene expression. *Proc. Natl. Acad. Sci. U.S.A.* **94**, 4582–4586 (1997).